

Supporting information

Power Generation, Evaporation Mitigation, and Thermal Insulation of Semitransparent Polymer Solar Cells: A Potential for Floating Photovoltaic Applications

Nan Zhang,[†] Guoliang Chen,[†] Yunxiang Xu,[†] Xiaofeng Xu,^{†,*} & Liangmin Yu^{‡,§}

[†]Department of Materials Science and Engineering, Ocean University of China, Qingdao 266100, China.

[‡]Key Laboratory of Marine Chemistry Theory and Technology, Ministry of Education, Ocean University of China, Qingdao 266100, China.

[§]Open Studio for Marine Corrosion and Protection, Pilot National Laboratory for Marine Science and Technology (Qingdao), China.

*Corresponding Author: X. Xu, e-mail: xuxiaofeng@ouc.edu.cn

Table of Contents

1. Materials.....	S2
2. Optical properties	S3
3. Electrochemical properties.....	S3
4. Tapping-mode atomic force microscopy (AFM) images	S5
5. SCLC mobility measurement	S5
6. Bimolecular recombination characterization	S7
7. <i>J–V</i> characteristics of the solar cells with different active areas	S7
8. Transmittance of the ST-PSCs	S10
9. Stability of the ST-PSCs	S10
10. Absorption coefficients of the pigments	S11
11. Infrared (IR) images of the water and films	S11
12. <i>J–V</i> characteristics of the ST-PSCs after 60 min illumination.....	S12
13. Reference.....	S13

1. Materials

PTB7-Th, PC₇₁BM, and ITIC purchased from Solarmer Energy, Inc. PNDI-T5 was synthesized by using a similar procedure according to previous literature.¹ Chlorophyll a, chlorophyll b, and xanthophyll were purchased from MREDA.

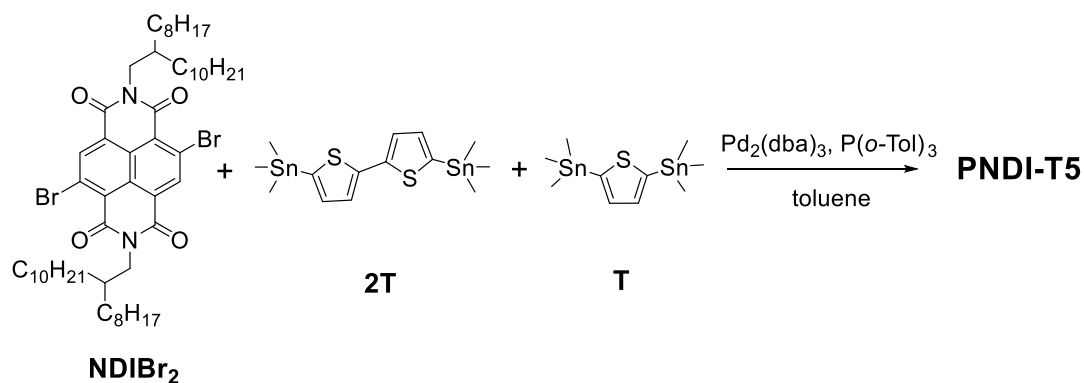


Figure S1. A synthetic route of the acceptor polymer PNDI-T5.

The 2,6-dibromonaphthalene-1,4,5,8-tetracarboxylic-*N,N'*-bis(2-octyldodecyl)diimide (NDIBr₂) (0.25 mmol, 246.3 mg), 5,5'-bis(trimethylstannyl)-2,2'-bithiophene (2T) (0.2375 mmol, 116.8 mg), 2,5-bis(trimethylstannyl)thiophene (T) (0.0125 mmol, 5.1 mg), tris(dibenzylideneacetone)dipalladium(0) (Pd₂(dba)₃) (4.58 mg) and tri(*o*-tolyl)phosphine (P(*o*-Tol)₃) (6.08 mg) were dissolved in anhydrous toluene (12 mL) under nitrogen atmosphere. The reaction mixture was heated at 100 °C with vigorous stirring for 2 h. Then, the trimethylstannyl-terminal groups were capped with 2-bromothiophene (0.05 mL) by refluxing for 1 h. After that, the bromo-terminal groups were capped with 2-(tributylstannyl)thiophene (0.1 mL) by refluxing for another 1 h. After cooling to room temperature, the polymer was precipitated by pouring the solution into acetone and was collected by filtration through a 0.45 μm Teflon filter. Then the polymer was washed in a Soxhlet extractor with acetone, diethyl ether, dichloromethane, and chlorobenzene (CB). The CB fraction was purified by passing it through a silica gel column and then precipitated from diethyl ether. Finally, the polymer was obtained by filtration through 0.45 μm Teflon filter and dried under vacuum at 40 °C for 24 h, which afforded 290.8 mg of PNDI-T5 with a yield of 79%. The number-average molecular weight

(M_n) is 62.5 kDa and polydispersity index (PDI) is 2.8.

2. Optical properties

Absorption and transmittance spectra were measured with a PerkinElmer Lambda 900 UV-Vis-NIR absorption spectrometer.

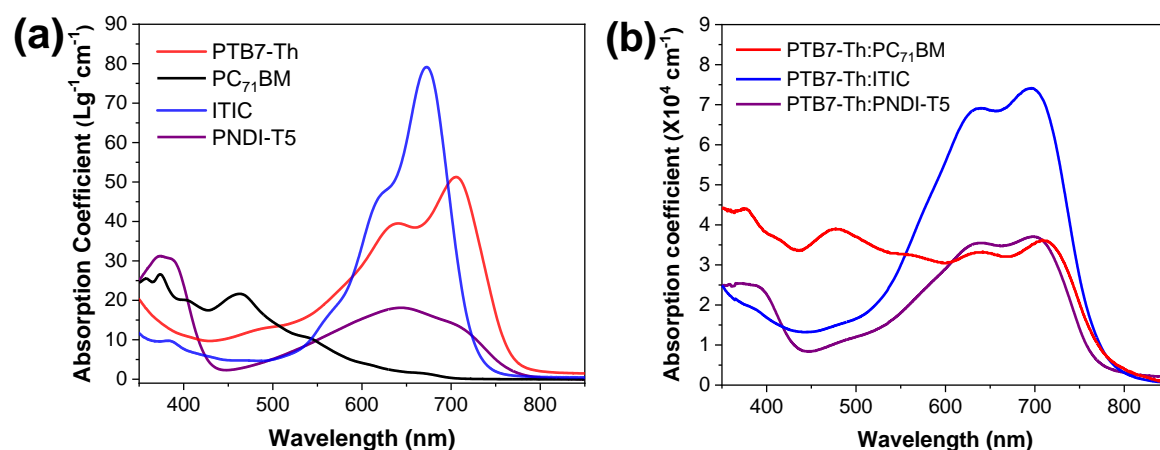


Figure S2. (a) Absorption coefficients of PTB7-Th, ITIC, PC₇₁BM, and PNDI-T5 in 1,2-dichlorobenzene (o-DCB); (b) absorption coefficients of the blend films.

3. Electrochemical properties

Square wave voltammetry (SWV) measurements were carried out on a CH-Instruments 650A Electrochemical Workstation. A three-electrode setup was used with platinum wires for both the working electrode and counter electrode, and Ag/Ag⁺ was used for the reference electrode calibrated with a ferrocene/ferrocenyl couple (Fc/Fc⁺). A 0.1 M nitrogen-saturated solution of tetrabutylammonium hexafluorophosphate (Bu₄NPF₆) in anhydrous acetonitrile was used as the supporting electrolyte. The polymer films were deposited onto the working electrode from the corresponding o-DCB solutions.

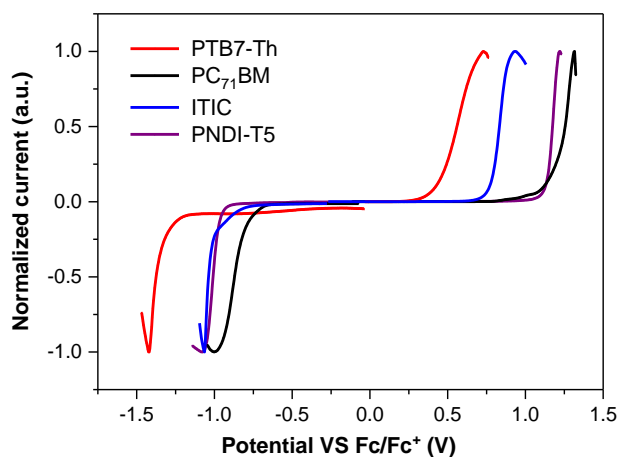


Figure S3. Square wave voltammetry measurements of PTB7-Th, PC₇₁BM, ITIC, and PNDI-T5.

The HOMO and LUMO levels were estimated from the peak potentials by setting the oxidative peak potential of Fc/Fc⁺ vs. the normal hydrogen electrode (NHE) to 0.63 V, and the NHE vs. the vacuum level to 4.5 V.²⁻³ The energy levels were calculated according to the formula $\text{HOMO} = -(E_{\text{onset,ox vs. Fc/Fc}^+} + 5.13) \text{ eV}$ and $\text{LUMO} = -(E_{\text{onset,red vs. Fc/Fc}^+} + 5.13) \text{ eV}$, where the E_{ox} and E_{red} were determined from the onsets of the oxidation and reduction peaks, respectively.

4. Tapping-mode atomic force microscopy (AFM) images

The surface morphology of the blend films were acquired by using tapping-mode atomic force microscopy (AFM, Agilent 5500) with MikroMasch NSC-15 AFM tips and resonant frequencies of 300 kHz.

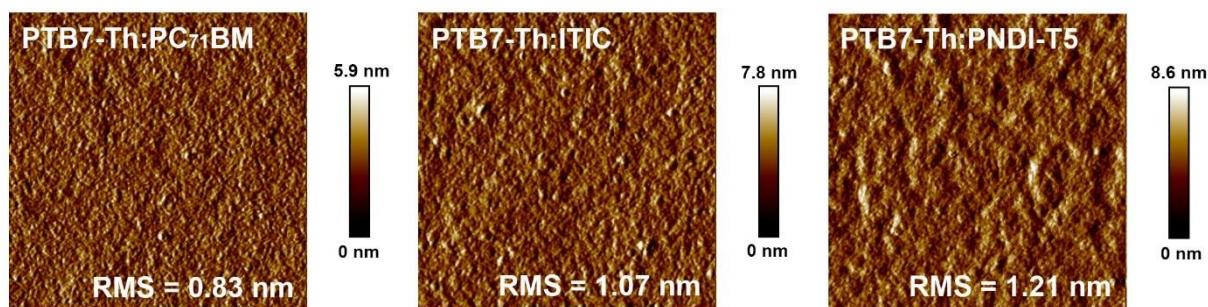


Figure S4. AFM topography ($2.5 \times 2.5 \mu\text{m}^2$) and root-mean-square (RMS) roughness of the blend films

5. SCLC mobility measurement

Hole mobility was measured in a hole-only device composed of ITO/PEDOT:PSS/active layer/MoO₃/Ag. The electron mobility was measured in an electron-only device composed of ITO/ZnO/active layer/PDINO/Ag. For the hole-only device, the blend films were spin-coated on ITO substrates covered with 40 nm PEDOT:PSS. The CB or o-DCB solutions of the blends were spin-coated at ~ 1000 rpm for 80 s in a glove box. After that, MoO₃ (8 nm) and Ag (80 nm) were successively vacuum-deposited on the active layers. For the electron-only device, sol-gel ZnO was spin-coated onto the ITO-coated glass at a spinning rate of 4000 rpm for 40 s, followed by thermal annealing at 150 °C for 30 min. The CB or o-DCB solutions of the blends were spin-coated on the layer of ZnO (40 nm) in a glove box. After that, the ethanol solution of PDINO was spin-coated at 3000 rpm for 25 s. Finally, Ag (80 nm) was vacuum-deposited on top of the PDINO layer (5 nm).

According to the Murgatroyd law and using the Equation (S1) to fit the trap-filled region of the J - V curves from the single carrier devices, SCLC mobilities was calculated in a precise way.⁴

$$J = \frac{9}{8} \varepsilon_r \varepsilon_0 \mu \frac{(V-V_{bi})^2}{L^3} \exp\left(\frac{0.89}{kT} \gamma \left(\frac{\sqrt{V-V_{bi}}}{\sqrt{L}}\right)\right) \quad (\text{S1})$$

where J is the current density, ε_r is the relative dielectric constant of the polymer blend ($\varepsilon_r = 3.6$), ε_0 is the free-space dielectric constant, μ is the temperature-dependent mobilities at zero field, L is the thickness of the active layer, $V-V_{bi}$ is the effective voltage, k is Boltzmann constant, T is the absolute temperature and γ is the field enhancement factor.⁵

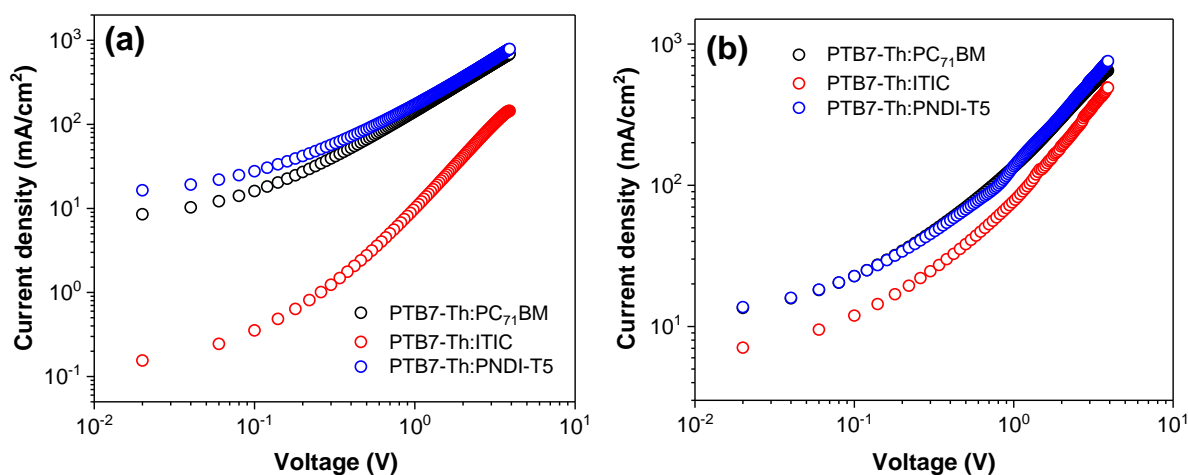


Figure S5. (a) Current density–voltage curves of the blend films with the hole-only device structure of ITO/PEDOT:PSS (40 nm)/active layer/MoO₃ (8 nm)/Ag (80 nm); (b) current density–voltage curves of the blend films with electron-only device structure of ITO/ZnO (40 nm)/active layer/PDINO (5 nm)/Ag (80 nm).

Table S1. Hole and electron mobilities of the solar cells.

active layer	μ_h (cm ² V ⁻¹ s ⁻¹)	μ_e (cm ² V ⁻¹ s ⁻¹)	μ_e/μ_h
PTB7-Th:PC ₇₁ BM	3.57×10^{-4}	3.39×10^{-4}	0.95
PTB7-Th:ITIC	2.12×10^{-4}	7.51×10^{-4}	3.54
PTB7-Th:PNDI-T5	6.38×10^{-4}	5.73×10^{-4}	0.90

6. Bimolecular recombination characterization

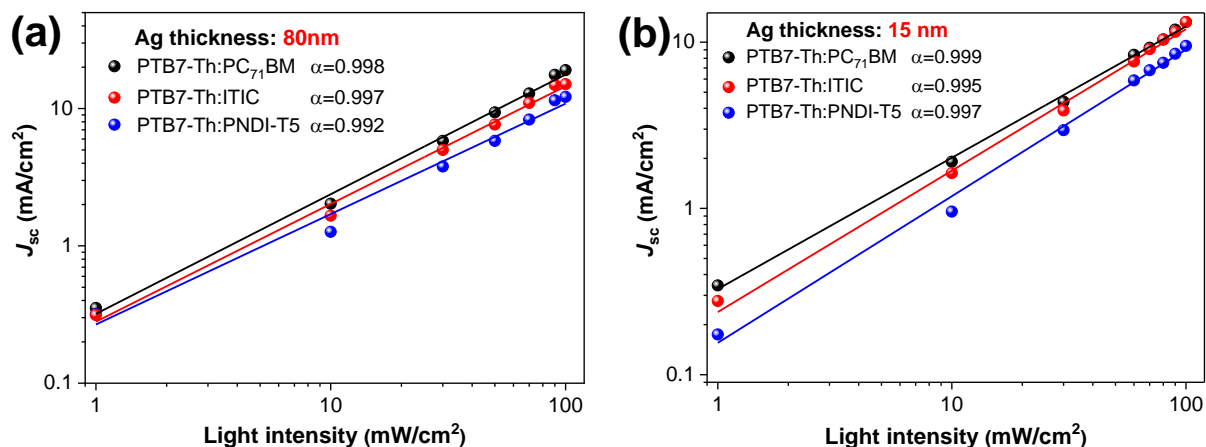
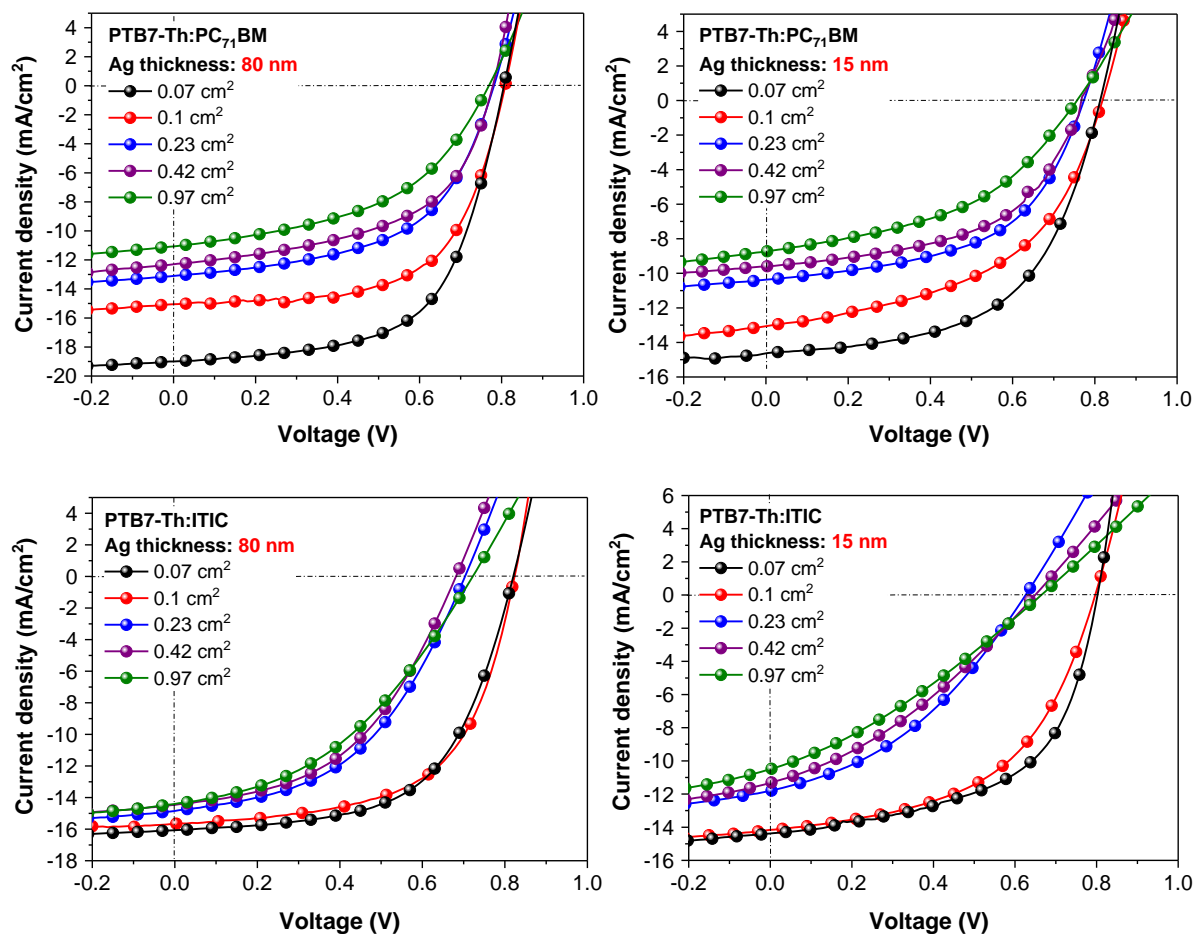


Figure S6. J_{sc} versus natural logarithm of the light intensity fitted by a linear relationship for the (a) opaque PSCs, and (b) ST-PSCs.

7. $J-V$ characteristics of the solar cells with different active areas



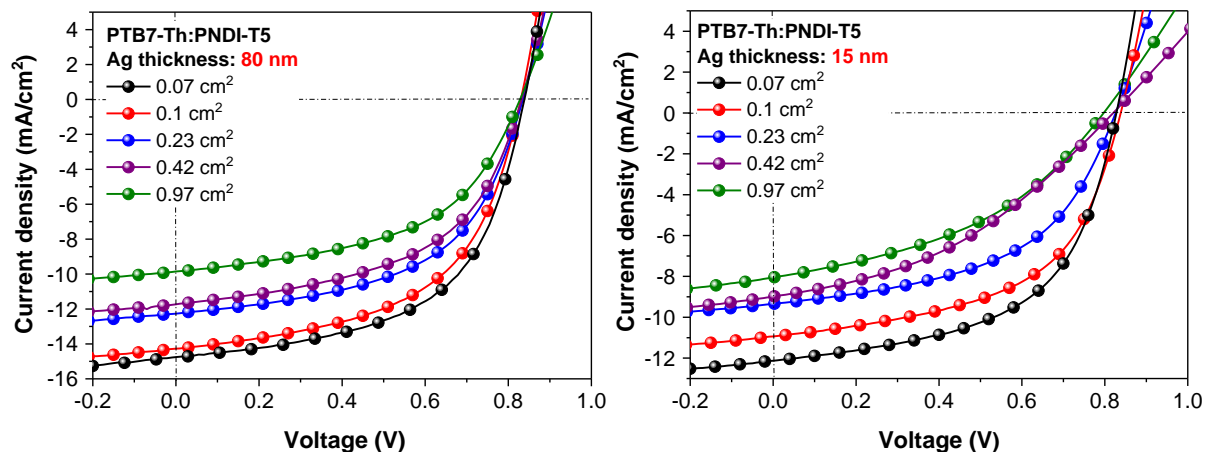


Figure S7. J - V curves of the PSCs with different device areas and Ag thickness (80 nm and 15 nm).

Table S2. Device parameters of the PSCs with different device areas (Ag thickness is 80 nm).

PSC	device area (cm ²)	V_{oc} (V)	J_{sc} (mA/cm ²)	FF	PCE (%)
PTB7-Th:PC ₇₁ BM	0.07	0.81	19.00	0.61	9.4 ^a (9.15±0.25) ^b
	0.10	0.81	15.05	0.62	7.6 (7.49±0.11)
	0.23	0.78	13.10	0.55	5.6 (5.47±0.13)
	0.42	0.78	12.30	0.54	5.2 (5.12±0.08)
	0.97	0.77	11.06	0.48	4.1 (4.03±0.07)
PTB7-Th:ITIC	0.07	0.82	16.20	0.63	8.4(8.27±0.13)
	0.10	0.82	15.64	0.62	8.0 (7.70±0.30)
	0.23	0.70	14.67	0.48	4.9 (4.76±0.14)
	0.42	0.68	14.40	0.47	4.6 (4.47±0.13)
	0.97	0.72	14.40	0.41	4.3 (4.28±0.02)
PTB7-Th:PNDI-T5	0.07	0.84	14.75	0.56	6.9 (6.63±0.27)
	0.10	0.83	14.25	0.55	6.5 (6.47±0.03)
	0.23	0.83	12.27	0.54	5.5 (5.54±0.06)
	0.42	0.83	11.73	0.52	5.1 (5.01±0.09)
	0.97	0.82	9.84	0.52	4.2 (4.15±0.05)

^aThe maximal PCE; ^bThe average PCE from 15 devices.

Table S3. Device parameters of the ST-PSCs with different device areas (Ag thickness is 15 nm).

ST-PSCs	device area (cm ²)	V _{oc} (V)	J _{sc} (mA/cm ²)	FF	PCE (%)
PTB7-Th:PC ₇₁ BM	0.07	0.81	14.64	0.56	6.7 ^a (6.58±0.12) ^b
	0.10	0.82	13.06	0.59	6.3 (6.17±0.13)
	0.23	0.77	10.37	0.54	4.3 (4.12±0.18)
	0.42	0.77	9.59	0.53	3.9 (3.81±0.09)
	0.97	0.76	8.69	0.45	3.0 (2.96±0.04)
PTB7-Th:ITIC	0.07	0.80	14.61	0.55	6.4 (6.29±0.11)
	0.10	0.80	14.12	0.53	5.9 (5.77±0.13)
	0.23	0.63	11.79	0.38	2.8 (2.68±0.12)
	0.42	0.65	11.30	0.33	2.4 (2.30±0.10)
	0.97	0.66	10.48	0.31	2.2 (2.13±0.07)
PTB7-Th:PNDI-T5	0.07	0.83	12.11	0.56	5.6 (5.46±0.14)
	0.10	0.84	10.92	0.55	5.0 (4.88±0.12)
	0.23	0.83	9.34	0.51	4.0 (3.93±0.07)
	0.42	0.82	8.98	0.39	2.9 (2.86±0.04)
	0.97	0.80	8.04	0.42	2.7 (2.65±0.05)

^aThe maximal PCE; ^bThe average PCE from 15 devices.

8. Transmittance of the ST-PSCs

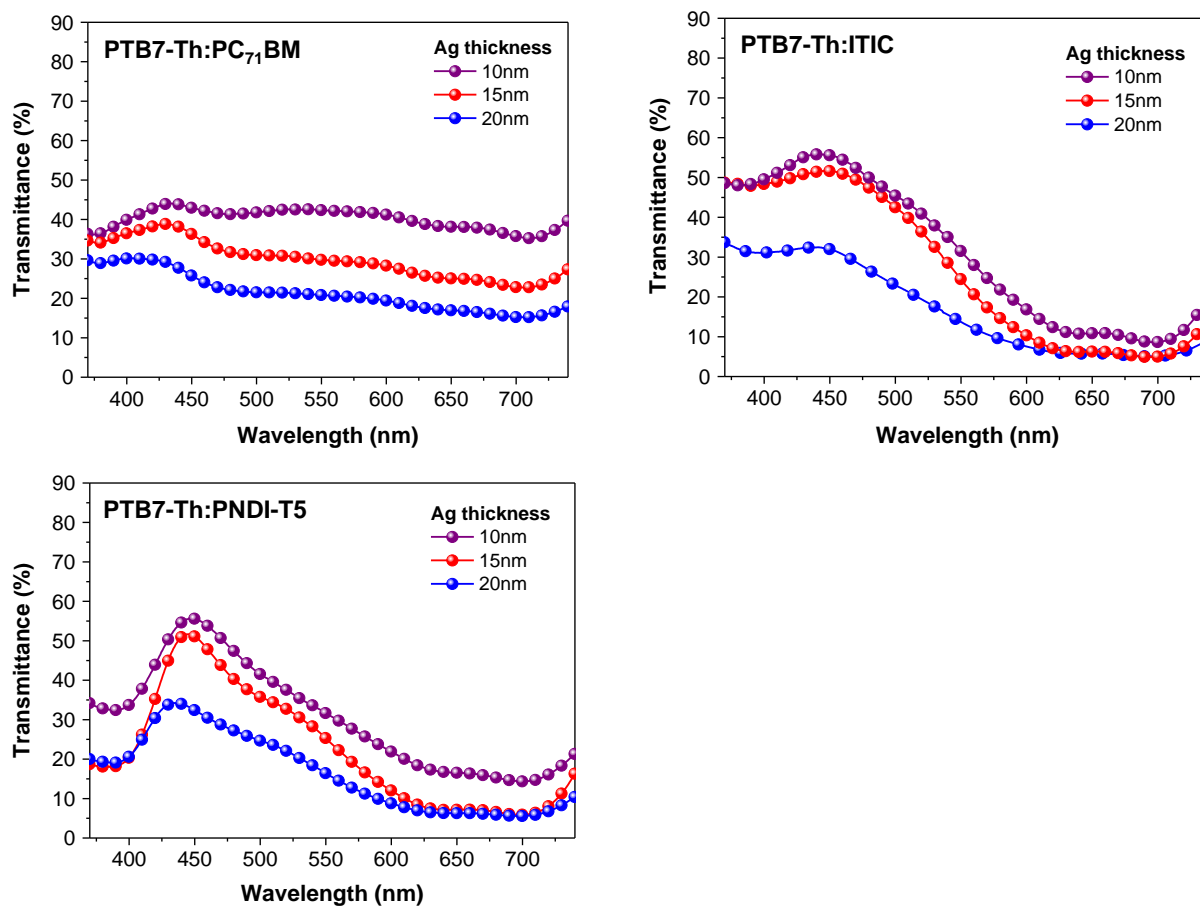


Figure S8. Transmittance spectra of the ST-PSCs with different Ag thickness from the anode side.

9. Stability of the ST-PSCs

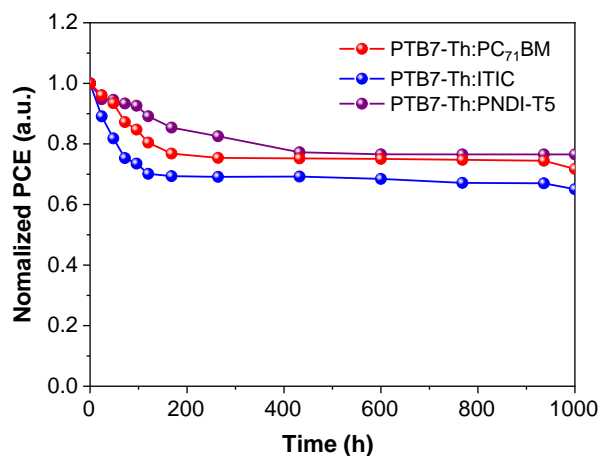


Figure S9. Stability of the encapsulated ST-PSCs in ambient atmosphere (average temperature of ~20 °C and relative humidity of ~30%).

10. Absorption coefficients of the pigments

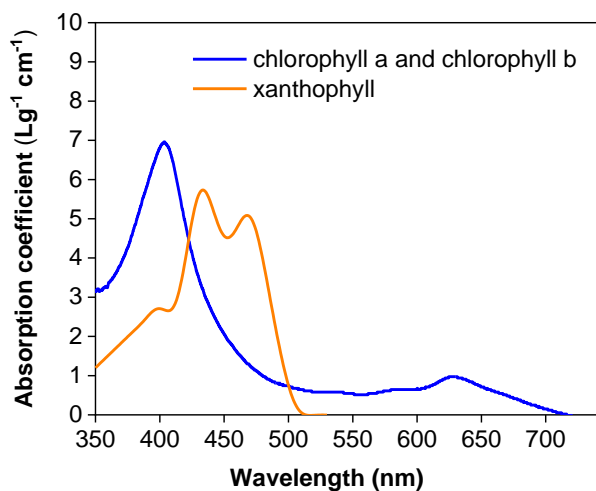


Figure S10. Absorption coefficients of the common light-absorbing pigments in algal cells.

11. Infrared (IR) images of the water and films

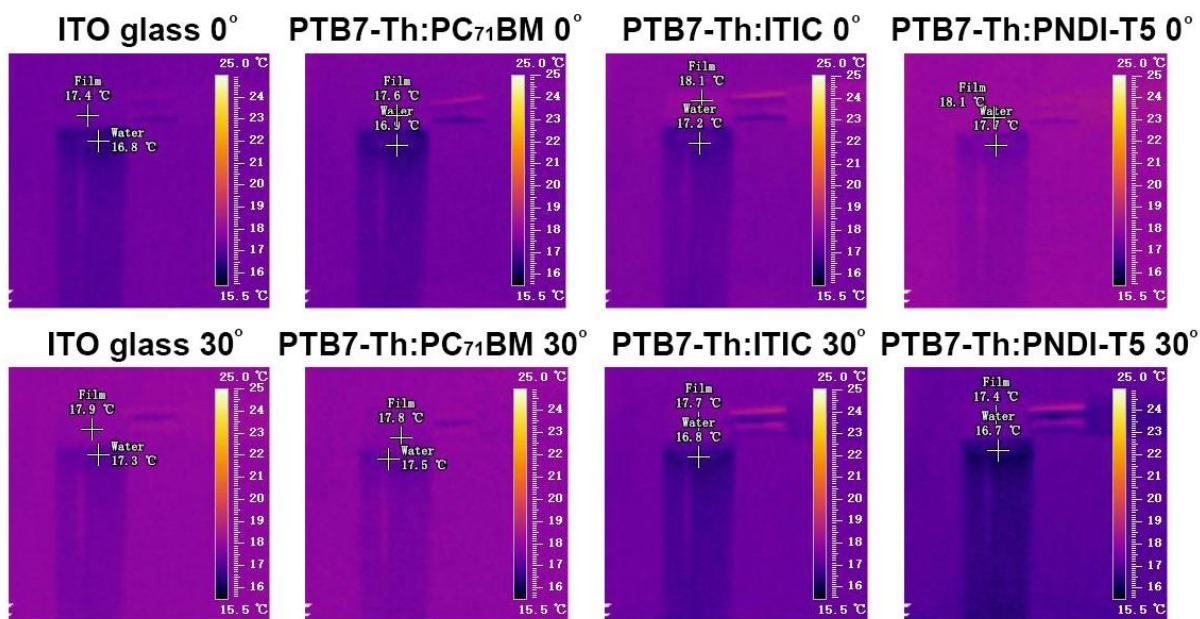


Figure S11. IR images and temperature profiles of the surface of the fresh water, ITO and ST-PSCs before sun irradiation.

12. J - V characteristics of the ST-PSCs after 60 min illumination

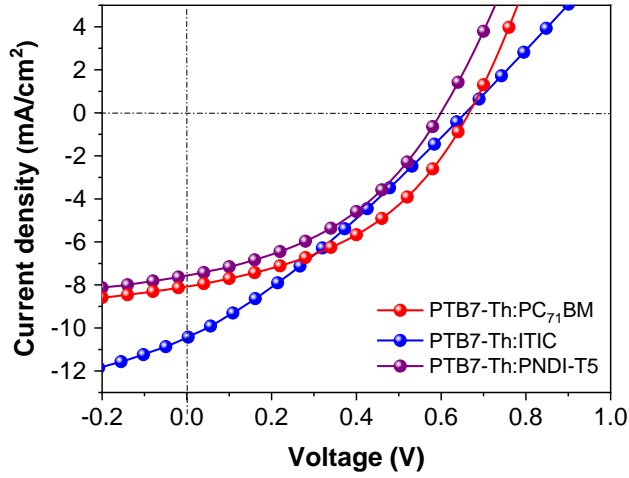


Figure S12. J - V curves of the ST-PSCs (active areas: 0.97 cm^2) after 60 min illumination under one sun (AM 1.5G, 100 mW/cm^2).

Table S4. Photovoltaic parameters of the ST-PSCs after 60 min illumination

ST-PSCs	V_{oc} (V)	J_{sc} (mA/cm^2)	FF	PCE (%)
PTB7-Th:PC ₇₁ BM	0.66	8.08	0.42	2.2
PTB7-Th:ITIC	0.65	10.41	0.28	1.9
PTB7-Th:PNDI-T5	0.60	7.53	0.41	1.9

13. Reference

- (1) Li, Z.; Xu, X.; Zhang, W.; Meng, X.; Ma, W.; Yartsev, A.; Inganäs, O.; Andersson, M. R.; Janssen, R. A. J.; Wang, E. High Performance All-Polymer Solar Cells by Synergistic Effects of Fine-Tuned Crystallinity and Solvent Annealing. *J. Am. Chem. Soc.* **2016**, *138* (34), 10935-10944.
- (2) Pavlishchuk, V. V.; Addison, A. W. Conversion Constants for Redox Potentials Measured versus Different Reference Electrodes in Acetonitrile Solutions at 25°C. *Inorg. Chim. Acta* **2000**, *298* (1), 97-102.
- (3) Cardona, C. M.; Li, W.; Kaifer, A. E.; Stockdale, D.; Bazan, G. C. Electrochemical Considerations for Determining Absolute Frontier Orbital Energy Levels of Conjugated Polymers for Solar Cell Applications. *Adv. Mater.* **2011**, *23* (20), 2367-2371.
- (4) Felekidis, N.; Melianas, A.; Kemerink, M. Design Rule for Improved Open-Circuit Voltage in Binary and Ternary Organic Solar Cells. *ACS Appl. Mater. Interfaces* **2017**, *9* (42), 37070-37077.
- (5) Murgatroyd, P. N. Theory of Space-Charge-Limited Current Enhanced by Frenkel Effect. *J. Phys. D: Appl. Phys.* **1970**, *3* (2), 151.